Turkish Journal of Electrical Engineering & Computer Sciences

http://journals.tubitak.gov.tr/elektrik/

Research Article

Turk J Elec Eng & Comp Sci
(2023) 31: 992 – 1005

doi:10.55730/1300-0632.4030

A unique hybrid domain hand-crafted feature to classify colorectal tissue histopathological images using multiheaded CNN

Anurodh KUMAR*, **Amit VISHWAKARMA**, **Varun BAJAJ**
Department of Electronics and Communication Engineering, PDPM Indian Institute of Information Technology Design and Manufacturing, Jabalpur, India

Received: 07.06.2023 • **Accepted/Published Online:** 19.09.2023 • **Final Version:** 27.10.2023

Abstract: Early diagnosis of colorectal cancer lengthens human life and is helpful in efforts to cure the illness. Histopathological inspection is a routinely utilized technique to diagnose it. Visual assessment of histopathological images takes more investigation time, and the decision is based on the individual perceptions of clinicians. The existing methods for colorectal cancer classification use only spatial information. However, studies on the spectral domains of information are lacking in the literature. Therefore, the performance of the existing techniques is moderate. To improve the performance of colorectal cancer classification, this work proposes a unique hybrid domain hand-crafted feature formulated using scale-invariant feature transform and mel-cepstrum domain features. The developed hand-crafted features use spatial as well as spectral information. Furthermore, the developed hand-crafted features are given as input to a newly developed 1D multiheaded convolutional neural network (1D MHCNN) for the classification of colorectal tissue utilizing histopathological images. The performance of the proposed network is compared with other existing methods. Based on the experiments, the proposed network performed with accuracy of 96.80%, specificity of 99.76%, precision of 97.12%, sensitivity of 96.64%, F1 score of 0.9688, and area under the curve of 0.9820. The proposed approach may be utilized to improve clinical diagnosis measurement performance.

Key words: Histopathological images, colorectal cancer, mel-cepstrum, multiheaded convolutional neural network, hand-crafted feature

1. Introduction

Colorectal cancer is a major cause of death globally according to global cancer statistics [1]. As per the American Cancer Society, there will be 53,000 colorectal cancer deaths and 1.53 million new cases in the United States in 2023 [2]. It originates in the large intestine. The most significant risk factors for colorectal cancer are polyposis, a lack of awareness, older age, inactive lifestyle, obesity, and family history of the disease. Early detection of it is a particularly essential clinical step in preventing and prolonging human lives [3]. Fecal occult blood is a stool-based assessment test that is followed by colonoscopy as a standard method to diagnose colorectal cancer, which facilitates a direct visual inspection of the entire rectum and colon. Despite scientific developments, the present manual inspection of colonoscopy findings is still tedious and time-consuming [4].

Medical imaging is a beneficial application that is widely utilized in the early detection of various health-related issues [5]. Histopathological inspection is an imaging technique that is commonly utilized for the detection of various types of cancer. However, histopathological diagnosis must be performed by a clinical

*Correspondence: 1912602@iiitdmj.ac.in

expert, it requires more inspection time, and the judgment is based on individuals' perceptions [6, 7]. Automated detection of colorectal cancer using artificial intelligence can increase diagnostic performance and provide a secondary option to clinicians in making their decisions [8]. Numerous computer-aided diagnosis-based systems have been reported in the literature to diagnose colorectal cancer. Takamatsu et al. [9] utilized a random forest algorithm for the early detection of colorectal cancer using digital slide images. Manual screening of tumor buds takes more time and the results may differ according to clinicians' differing perceptions [10]. Weis et al. [10] proposed a machine learning-based model for the detection of tumor buds using histopathological images. A deep learning (DL)-based algorithm has also been used to automatically extract features from the raw input [11]. This is a useful method for detecting various kinds of health issues. The convolutional neural network (CNN) is a commonly utilized DL architecture. Shaban et al. [12] suggested a context-aware CNN-based framework for grading colorectal cancer using histological images. Kwak et al. [13] developed a DL-based architecture to detect lymph node metastases for the detection of colorectal cancer using histopathological images.

2. Related work

Altunbay et al. [14] developed a color graph approach for diagnosing colon cancer using histopathological images. They extracted a set of structural features using a color graph technique. The extracted features were given as input to the support vector machine (SVM) classifier for the classification of colon cancer stages. They performed evaluations of 213 micrographs of colorectal tissue histopathological images. In [14], the authors utilized 18 color graph features and attained an accuracy rate of 82.65%. They claimed that they utilized the color graph technique for diagnosing cancer for the first time. Olgun et al. [15] decomposed histopathological images into their constituents of eosin and hematoxylin. Using these constituents, the authors produced a set of feature descriptors named local object patterns. They defined descriptors utilizing the idea of local binary patterns. They performed experiments on 3226 histopathological images of the colon tissues of 258 patients. An overall accuracy rate of 93% was achieved. Rathore et al. [16] suggested a hybrid feature space-based algorithm to diagnose colon cancer. They utilized hybrid features for discriminating between malignant and normal colon samples. For the development of hybrid features, these authors used scale-invariant feature transform (SIFT), texture, and morphological features [16]. They utilized different kernels of the SVM classifier and tested the experimental performance on 174 histological images. They achieved accuracy of 92.53%.

Zhao et al. [17] developed an integrated model (logistic regression and SVM) to classify colorectal cancer. They utilized the data normalization technique to scale feature values. They applied radial basis function (RBF), sigmoid, polynomial, and linear kernels in the SVM to compare the performance of the network. From among these kernels, RBF outperformed the others. An accuracy rate of 91.2% was achieved using a learning rate of 0.01 and 100 iterations. Masud et al. [18] applied discrete wavelet transform and discrete Fourier transform techniques to extract the features to classify colon cancer utilizing histopathological images. Four sets of features were extracted using these two transform methods. Furthermore, the resultant features were combined to create a new set of features. The authors used unsharp masking as a preprocessing step to improve image quality. A spatially constrained CNN was used to detect and classify colorectal cancer nuclei [19]. To locate and identify colorectal cancer nuclei, their method did not require nuclei segmentation. To classify the nuclei, the authors proposed a neighbor ensemble predictor integrated with the CNN to more accurately predict the class labels of detected nuclei. Twenty thousand annotated nucleus images from four categories were used to test the performance.

The Riezs transform was suggested by Yazdi et al. [20] for the classification of colorectal cancer. These authors utilized geometry and texture-based features to show the variability in histopathological images. The extracted features were given as input to the SVM classifier. They achieved a classification accuracy of 93.40%. A bilinear CNN was proposed by Wang et al. [21] to classify multiclass colorectal tissue. To learn more appropriate features, these authors decomposed histopathological images into eosin and hematoxylin components. The authors performed their analysis on 1000 nonoverlapping histological images. They achieved accuracy of 92.6%. To classify multiclass colorectal tissue histopathological images, Ghosh et al. [22] utilized an ensemble deep neural network (EDNN). Their developed network was compared with three benchmark models (Xception, Inception-ResNetV2, and DenseNet121), which were trained on ImageNet. The authors used the Adam optimizer to train all CNNs with 30 epochs and a batch size of 64. Hamida et al. [23] developed a DL-based procedure to identify and classify regions of colorectal cancer using sparsely annotated histopathological data. They used a data augmentation approach to boost training samples and compared their proposed network to five benchmark models (VGG, ResNet, Inception, AlexNet, and DenseNet). In the comparisons of the models, ResNet performed better.

A transfer learning (TL)-based approach was utilized by Ohata et al. [24] to classify colorectal cancer using histopathological images. The features were extracted using various CNNs through a TL approach. The extracted features were given to various traditional classifiers. Compared to other networks, DenseNet169 integrated with SVM (RBF) attained an accuracy rate of 92.08%. To classify multiclass colorectal tissue histopathological images, Kumar et al. [25] proposed CRCCN-Net. These authors compared the computational time of various DL-based models. They used the Adam optimizer to train the network. In [25], dropout of 0.2 was utilized to prevent the network from becoming overfit. Liang et al. [6] developed a multiscale feature fusion CNN (MFFCNN) based on shearlet transform to identify colon cancer using histological images. Shearlet transform is an image analysis method based on affine transform and it can be used to find singularities in an image with multiple scales. The shearlet coefficients include details such as edges and contours. A TL-based approach was also applied by Kather et al. [26] to evaluate the microenvironment of tumors using histopathological images. Five pretrained networks, namely GoogleNet, AlexNet, VGG19, SqueezeNet, and ResNet50, were tested for performance analysis. In comparison to other pretrained models, VGG19 achieved better classification performance.

Most of the above-reported techniques for colorectal tissue classification based on histopathological images use only spatial information; the frequency domains of information are not taken into account. As a result, the existing models' performance is average. Furthermore, it is noted that various techniques have been applied to balanced datasets and binary classifications of colorectal tissue. Moreover, few types of techniques have been proposed to classify multiclass colorectal tissue. Most of the DL-based techniques to classify colorectal tissue have large sizes. These models require more testing and training time because there are more learnable parameters in them. As a result, these models' classification performance is average. For improving colorectal tissue classification performance, this study proposes a hybrid combination of unique hand-crafted features using SIFT and 2D mel-cepstrum domain features. The proposed integrated hand-crafted features classify colorectal tissue using both spatial and spectral information. Furthermore, the proposed approach is created in such a way that the model's capacity is nearly ideal because the accuracy differs between training and testing by 1.5% and both accuracies are higher than 96%. The new contributions of this work include the following:

- To denoise images while preserving high-frequency details, such as edges, nonlocal mean-based preprocessing has been used.
- We propose a unique hand-crafted feature formulated using image, SIFT, and 2D mel-cepstrum domain features for the classification of colorectal tissue.
- A new 1D multiheaded CNN (1D MHCNN) is developed that reads and interprets additional information from input features at distinct resolutions.

The rest of this study is organized as follows: following the discussion of the related work here in Section 2, materials and methods are addressed in Section 3, results and a discussion are presented in Section 4, and conclusions are offered in Section 5.

3. Materials and methods

3.1. Dataset

The dataset [27] consists of 100K histopathological images of normal and colorectal cancer tissues. Each class has a different number of images. The size of each image is 224 x 224 pixels. There are nine classes in this dataset. These nine classes are debris (DEB), lymphocytes (LYM), colorectal adenocarcinoma epithelium (TUM), mucus (MUC), adipose (ADI), smooth muscle (MUS), normal colon mucosa (NORM), background (BACK), and cancer-associated stroma (STR). Out of the total images, the DEB class has 11,512 images, the LYM class has 11,557 images, the ADI class has 10,407 images, the TUM class has 14,317 images, the MUS class has 13,536 images, the MUC class has 8896 images, the NORM class has 8763 images, the BACK class has 10,566 images, and the STR class has 10,446 images. Figure 1 shows a sample image from each class.

3.2. Preprocessing utilizing nonlocal mean (NLM) filter

NLM is an image-denoising method in image processing. The NLM filter proposed by Buades et al. [28] is easy to implement and excels at effectively removing additive noise while preserving edges. The NLM filter performs well for macroscopic imaging like magnetic resonance and computed tomography [29]. However, the NLM filter has not yet been utilized for the diagnosis of colorectal cancer with histopathological images in the literature. This study applies the NLM filter to minimize the effect of noise from histopathological images because the NLM filter excels at effectively removing noise while preserving edges. Mathematically, the NLM algorithm is expressed as follows [28]:

$$u(i) = NLM(f) = \frac{1}{\bar{w}(i)} \int_{\Omega} f(j) w(i,j) dj \tag{1}$$

Here, $\bar{w}$ is expressed as:

$$\bar{w}(i) = \int_{\Omega} w(i,j) dj \tag{2}$$

In Eq. (2), $w(i,j)$ is denoted as a weight that calculates the comparability of f between a neighbor of i and j and is defined as follows:

$$w(i,j) = exp(-\frac{d_l(f(i),f(j))}{m^2}) \tag{3}$$

Here, $i \in \Omega$, $j \in \Omega$, and d_l is defined as $d_l(f(i), f(j)) =$

$$\int_{\Omega} G_l(t) \left| f(i+t) - f(j+t) \right|^2 dt \tag{4}$$

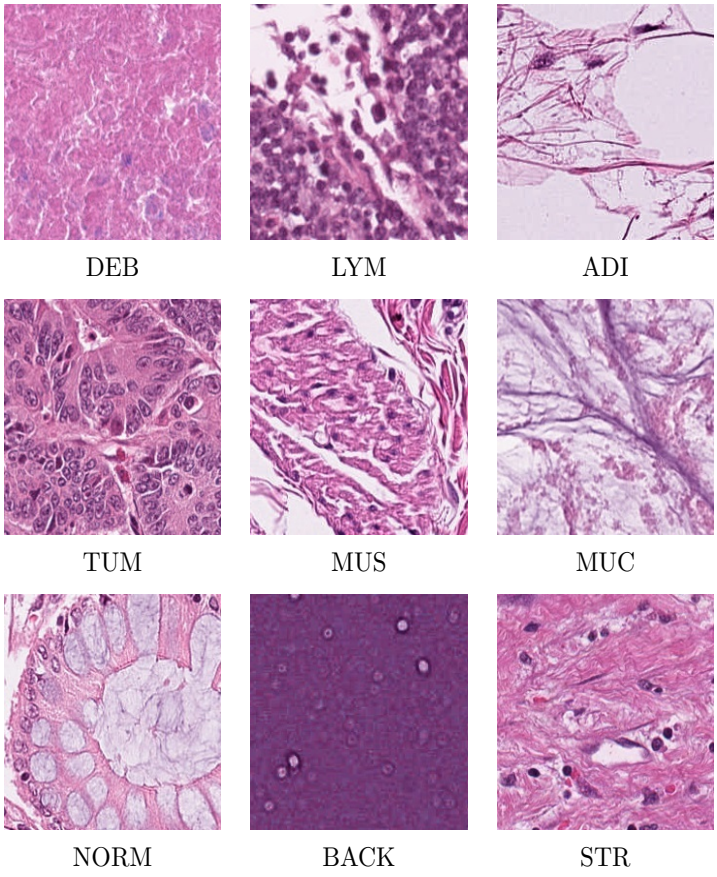

Figure 1. Class-wise images of normal and colorectal tissues from the dataset.

m in Eq. (3) denotes the controlling parameter of the decay of the weight. u is the denoised image for f. In Eq. (4), the Gaussian kernel G_l has a standard deviation of l.

3.3. Proposed unique hand-crafted feature

The extraction of useful features is necessary for image processing applications. However, depending on the image problem, the effective features may differ. To classify colorectal tissue utilizing histopathological images, this work proposes a unique hand-crafted feature. The proposed features are formulated using image, SIFT, and 2D mel-cepstrum domain features.

3.3.1. SIFT

SIFT is used to identify local, translation, scale, and rotation invariant features in images. The primary step involves finding key points in the scale space by concentrating on image locations that coincide with the maximum or minimum of the difference-of-Gaussian function. The scale space of a histopathological image [30] is expressed as the function $S(x, y, \alpha)$ that is acquired from the convolution of the input image, $I(x, y)$, and a variable-scale Gaussian, $G(x, y, \alpha)$:

$$S(x, y, \alpha) = G(x, y, \alpha) * I(x, y), \tag{5}$$

with

$$G(x,y,\alpha) = \frac{1}{2\pi\alpha^2} e^{\frac{-(x^2+y^2)}{2\alpha^2}} \tag{6}$$

Here, α denotes the standard deviation (SD) of the Gaussian $G(x,y,\alpha)$. The difference-of-Gaussian function $D(x,y,\alpha)$ can be evaluated from the difference of the Gaussians of two scales separated by factor d:

$$D(x,y,\alpha) = (G(x,y,d\alpha) - G(x,y,\alpha)) * I(x,y) = S(x,y,d\alpha) - S(x,y,\alpha) \tag{7}$$

The potential of SIFT to produce a large number of features that densely cover the image on all scales and locations is its main benefit.

3.3.2. 2D mel-cepstrum

Mel-cepstrum has been employed in a variety of domains, including seismology, speech analysis, and others [31, 32]. The mel-cepstrum feature for classifying images has been used in a few works in the literature. However, no study using mel-cepstrum features to classify colorectal tissue histological images has been reported yet in the literature. The 2D cepstrum gives features that are unconstrained in terms of scale invariance or gray-scale changes, which results in robustness against changes in illumination variations. The mel-cepstrum of an image contains more specific information about the image [32]. This comprehensive information may be useful for classifying multiclass colorectal tissue. The 2D mel-cepstrum $\hat{f}(s,t)$ of an image $I(x,y)$ is given as follows [31]:

$$\hat{f}(s,t) = F^{-1}(log(|Z(s,t)|^2)) \tag{8}$$

Here, (s,t) represents the 2D cepstral quefrency coordinates, F^{-1} represents inverse discrete Fourier transform, and $Z(s,t)$ is the discrete Fourier transform of the image. The 2D form of $\hat{f}(s,t)$ is converted to 1D $\hat{f}(x)$ by concatenating the columns of $\hat{f}(s,t)$ to make a single column, which will act as one of the components of the proposed combined feature vector. In this study, the SIFT and 2D mel-cepstrum domain features are denoted as $S(x,y)$ and $\hat{f}(s,t)$, respectively. Figure 2 shows some sample images of the dataset, highlighting the corresponding SIFT and mel-cepstrum of each image. From Figure 2 it can be seen that the mel-cepstrum and SIFT have different visual representations of four different classes of colorectal tissue histopathological images.

Algorithm 1. Algorithm for the developed unique hand-crafted features.

1: Input: Histopathological images $I(x \times y)$
2: I_pre: Convert denoised histopathological images RGB to gray
3: 2D image features extracted from $I(x,y)$
4: 2D $S(x,y)$ features extracted from $I(x,y)$ [using Eq. (5) to Eq. (7)]
5: 2D $\hat{f}(s,t)$ features extracted from $I(x,y)$ [using Eq. (8)]
6: 2D features obtained in steps 3 to 5 converted into respective 1D features by concatenating column of 2D features
7: Final concatenated 1D feature obtained using Eq. (9)

To produce unique hand-crafted features, the following procedures need to be applied. First, the denoised histopathological images are converted to their corresponding 1D features. To do this, an image is first converted into a gray-scale image. After that, the gray-scale image's columns are concatenated to develop a 1D feature. Utilizing the same procedure, the 2D SIFT (using Eq. (5) to Eq. (7)) and 2D mel-cepstrum (using Eq. (8)) of

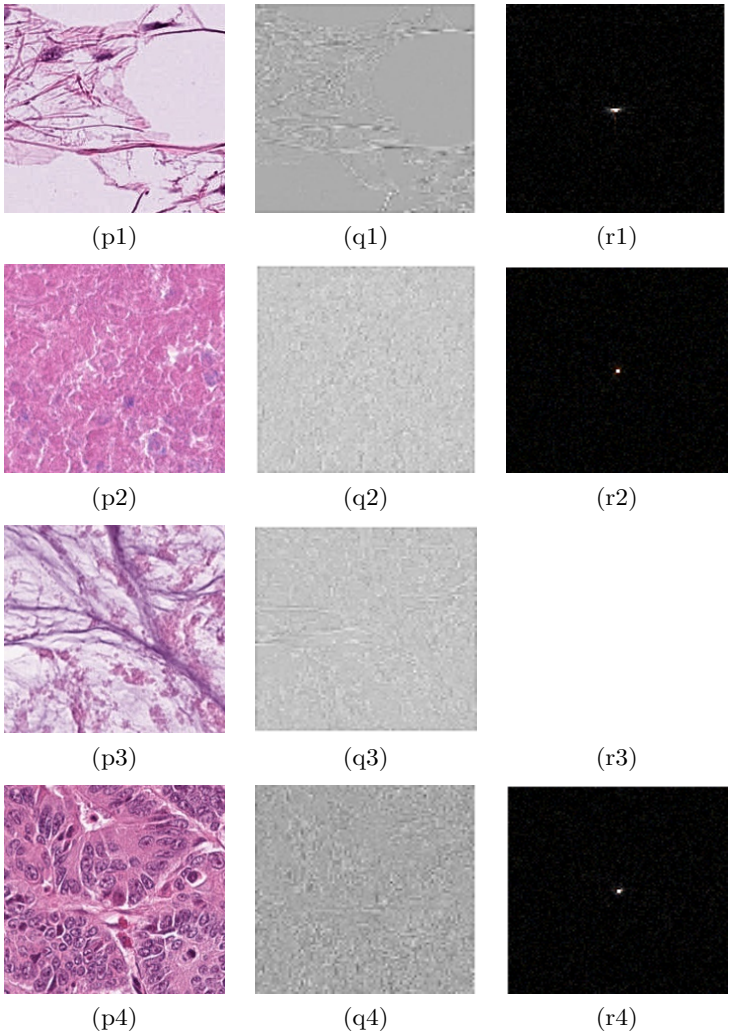

Figure 2. Images (pi) representing colorectal tissue, images (qi) depicting SIFT information, and images (ri) showing 2D mel-cepstrum descriptions. i varies from 1 to 4.

the same image are converted into a 1D feature. Afterwards, a combined feature of an image is generated by concatenating the 1D image feature, 1D $S(x,y)$ feature, and 1D $\hat{f}(s,t)$ feature. For better clarification about the development of the combined features, this process is shown in Figure 3. The final concatenated feature $Z(k)$ represented by Eq. (9) is a concatenation of the 1D form of the source image $I(x,y)$, mel-cepstrum image $\hat{f}(s,t)$, and SIFT image $S(x,y)$ domain features. The concatenated feature vector $Z(k)$ of an image $I(x,y)$ is obtained utilizing Eq. (5) to Eq. (8) as follows:

$$Z(k) = \text{1D feature: Concatenation of } S(x,y), \hat{f}(s,t) \tag{9}$$

From each image, 50,176 $\times$ 1 dimensions of features are obtained individually using an image, SIFT, and mel-cepstrum. Therefore, after the concatenation of each domain of features, we obtain 3 $\times$ 50,176 $\times$ 1 dimensions of the features from each image. The same process is used for all other histopathological images to develop

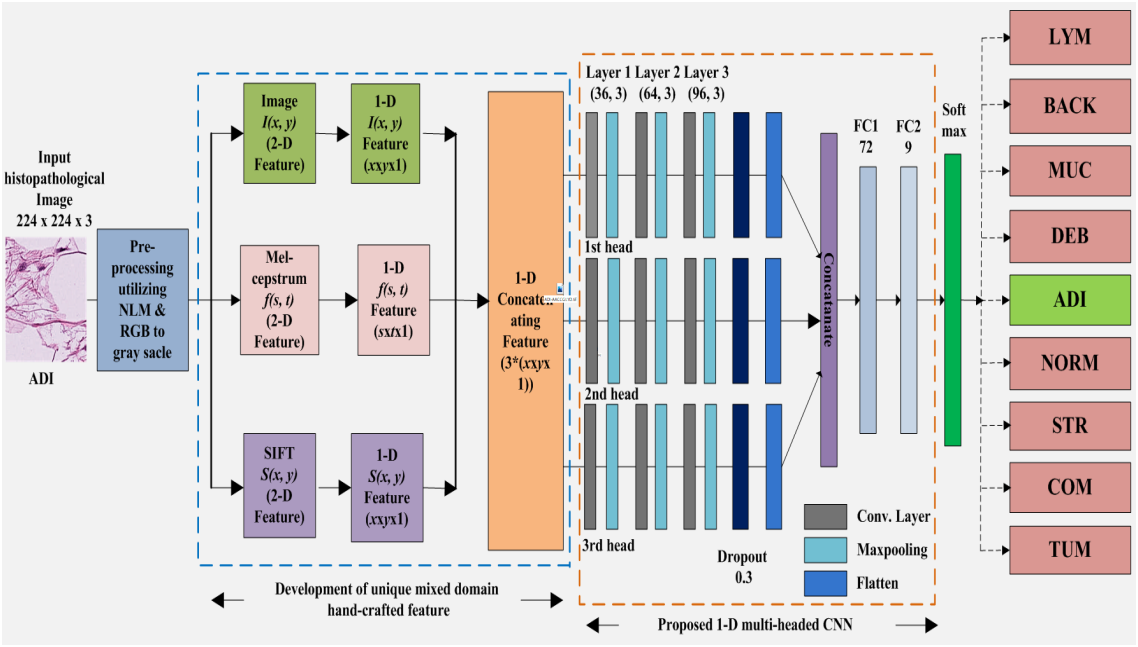

Figure 3. Illustrative representation of proposed technique to classify colorectal tissue histopathological images.

unique hand-crafted features. The concatenated feature (using Eq. (9)) is given as input to the newly proposed 1D MHCNN to classify multiclass colorectal tissue histopathological images. The process for developing unique hand-crafted features is shown in Algorithm 1.

3.4. Proposed 1D MHCNN

In the last decade, 2D CNNs have been widely used in numerous applications including computer vision, image classification, and object detection [11, 12, 25]. Most of the existing CNNs for the classification of colorectal cancer have more learnable parameters, many hidden layers, larger sizes, and higher weights. Therefore, these networks may not always give the best performance. To alleviate this issue, this study utilizes a 1D CNN. A real-time, low-cost hardware implementation is another benefit of using a 1D CNN because of its simple and compact design. The computational complexity of the 1D CNN is lower compared to the 2D CNN. 1D CNNs are frequently utilized for 1D signals for speech recognition, bearing fault detection, healthcare, and so on [33, 34]. They have many layers, including a fully connected layer (FCLr), a convolutional layer (CLr), a pooling layer (PLr), and a nonlinear transform layer. The effectiveness of networks is impacted by the utilization of learnable filters. Mathematically, a 1D CNN is expressed as follows [35]:

$$x_i^m = b_i^m + \sum_{j=1}^{N_{m-1}} Conv1D\left(W_{ji}^{m-1}, S_j^{m-1}\right) \tag{10}$$

Here, x_i^m denotes input data, b_i^m denotes the bias term of the i^{th} neuron at layer m, and S_j^{m-1} denotes the output of the j^{th} neuron at layer $m-1$. W_{ji}^{m-1} represents the kernel from the j^{th} neuron at layer $m-1$ to the i^{th} neuron at layer m.

Table 1. Total learnable parameters utilized in the proposed 1D MHCNN.

S.N.	Layer	Quantity of filters	Filter size	Total learnable parameters
1	Conv1D	36	3, 5, 7	1008
2	maxpooling1D	-	2x1	0
3	Conv1D	64	3, 5, 7	20,800
4	maxpooling1D	-	2x1	0
5	Conv1D	96	3, 5, 7	55,392
6	maxpooling1D	-	2x1	0
7	Dropout (0.3)	-	-	0
8	Flatten	-	-	0
9	Concatanate	-	-	0
10	FC1	-	-	5,419,080
11	FC2 Softmax	-	-	657

To improve the classification performance of colorectal tissue histopathological images, this study proposes the 1D MHCNN. The MHCNN consists of many heads. Each head of the network uses a distinct kernel size to read and interpret the input features in the proposed 1D MHCNN. The proposed network utilizes three heads, which have three distinct sizes of kernels: 3×1, 5×1, and 7×1. The multiple kernel sizes enable the model to read, understand, and analyze data at three distinct resolutions. The proposed network has three CLrs and three PLrs at each head. Each head of the first, second, and third CLr uses 36, 64, and 96 filters, respectively. The CLrs at every head are padded to ensure that the features map in the output that precisely matches the inputs. The PLr uses the max-pooling approach to decrease the parameters while maintaining essential information.

Relu is applied at each head of the CLr to enhance the network's nonlinearity. After three CLrs and PLrs, a flattening layer at each head integrates the output into a feature vector. Then a unique set of features is created by concatenating the feature interpretations from each head. The two FCLrs pass the resulting features. There are 72 neurons in the FC1 layer. In FC2, the number of neurons is 9. Each output node associates a class with a score for that class. The softmax layer converts scores from the layer before it into probabilities. The probabilities of the softmax layer are also utilized to compute the loss and select the predicted class during training and testing. In the proposed network, the number of CLrs, kernel size, and number of filters are tuned utilizing a grid-search algorithm. Figure 3 depicts the proposed network's layered architecture.

4. Results and discussion

The following steps are involved in classifying multiclass colorectal tissue. All histopathological images are first denoised utilizing the NLM filter and converted to gray-scale images. Second, a unique hand-crafted feature is developed using $I(x,y)$, $S(x,y)$, and the $\hat{f}(s,t)$ domain feature. Finally, the developed feature is given as input to the 1D MHCNN. To evaluate the outcomes of the proposed network, the following metrics are assessed: precision (Prec), sensitivity (Sens), accuracy (Accr), F1 score, specificity (Spec), and area under the curve (AUC). The mathematical formulas of these metrics are given in [36].

Among the total number of images, 80% are utilized for training, 12% for testing, and 8% for validation. The Adam optimizer is used to train the proposed network. The proposed 1D MHCNN is trained to 30 epochs with a batch size of 32. To prevent the network from overfitting [37], a dropout of 0.3 is used before the

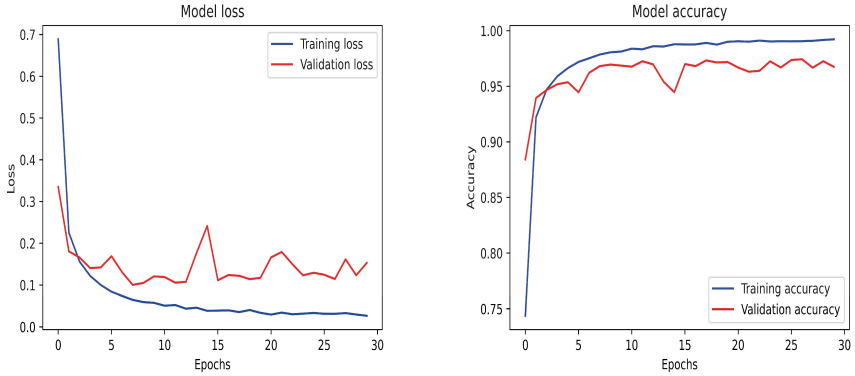

(a) (b)

Figure 4. (a) Representation of the proposed network's training and validation loss and (b) depiction of the proposed network's training and validation accuracy.

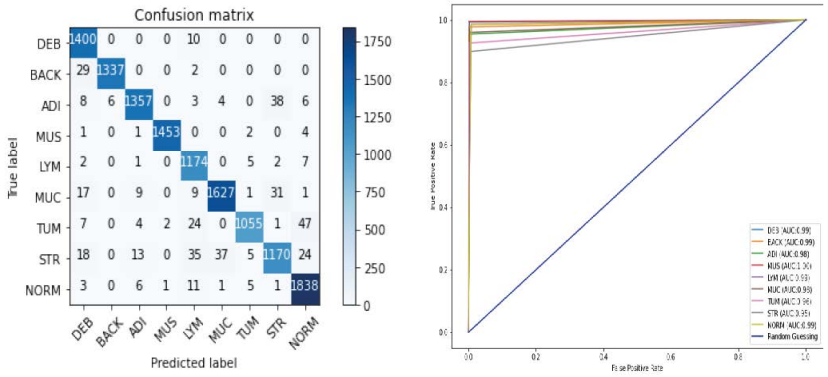

(a) (b)

Figure 5. (a) Representation of the confusion matrix obtained from test data using the NLM filter and (b) receiver operating characteristic curve of the proposed network.

flattened layer at each head of the network. The necessary layers are listed in Table 1, along with the total tunable parameters for every layer. In the proposed network, there are approximately 5.49 million learnable parameters used. The plots in Figure 4 show the network's training process. The plots in Figure 5 show the confusion matrix and receiver operating characteristic curve. Table 2 shows the test dataset outcomes for the proposed network architecture. Table 2 indicates that the proposed network has a more prominent impact on the test dataset for histopathological images using NLM.

The results above show that multiclass colorectal tissue can be classified using histopathological images more accurately when spatial and cepstrum domain features are combined. To assess the performance of the proposed 1D MHCNN, the Accr, Sens, Prec, Spec, F1 score, and AUC metrics are compared with those of other existing methods. To assess the efficacy of the proposed network, four recent notable colorectal tissue classification methods are compared on the same dataset: TL [26], MFFCNN [6], EDNN [22], and CRCCN-Net [25]. Table 3 compares the efficacy of the proposed approach with that of other recent techniques. Kather et al.

Table 2. Performance analysis of proposed network on test dataset using a concatenation of image, SIFT, and mel-cepstrum domain features.

Metrics	Without NLM	With NLM
Accr (%)	96.24 ± 0.4	96.80 ± 0.5
Prec (%)	96.64 ± 0.6	97.12 ± 0.3
Sens (%)	96.18 ± 0.3	96.64 ± 0.3
Spec (%)	99.24 ± 0.3	99.76 ± 0.4
F1 score	0.9640 ± 0.06	0.9688 ± 0.08
AUC	0.9766 ± 0.04	0.9820 ± 0.04

[26] utilized the TL approach to classify colorectal tissue. They used various benchmarking networks. Among other benchmarking networks, VGG19 achieved Prec of 94.33%, Sens of 92.33%, Accr of 94.30%, and Spec of 99.44%. They achieved the best AUC of 0.9950. Misclassifications between the STR, MUS, DEB, and LYM classes were most prevalent in [26]. The technique developed by Liang et al. [6] achieved Accr of 96.00%, Sens of 94.50%, F1 score of 0.9554, Prec of 97.42%, AUC of 0.9600, and Spec of 97.50%. The method proposed in [6] has an overfitting issue, so its performance is relatively low compared to others.

The EDNN was developed by Ghosh et al. [22] to classify multiclass colorectal tissue histopathological images. In [22], Prec of 96.17%, Spec of 96.17%, Accr of 96.16%, Sens of 96.15%, F1 score of 0.9610, and AUC of 0.9616 were achieved. That study was limited by the fact that ensembling may be space- and time-consuming. For some types of colorectal tissue, misclassification was also common. Their method provided the third-best performance. The method proposed by Kumar et al. [25] achieved Accr of 96.26%, Prec of 96.44%, Sens of 96.34%, Spec of 99.52%, AUC of 0.9800, and F1 score of 0.9638. Although their method provided promising results, misclassification was common among some classes of colorectal tissue. Their method provided the second-best results.

The proposed approach typically comprises three steps. First, the histopathological images are denoised using the NLM filter. NLM efficiently eliminates noise while preserving the edges of the image. Second, unique hand-crafted features are developed using a concatenation of spatial and cepstrum domain features. Due to the hybrid nature of feature vectors, the network may have less tendency to become overfit. Finally, the developed concatenated features are given as input to the proposed network to classify colorectal tissue utilizing histopathological images. In the proposed 1D MHCNN, each head of the network reads and interprets the input features using three different kernel sizes. The variations in kernel size allow the model to read, understand, and interpret data at three different resolutions. Furthermore, the proposed approach is built so that the model's capacity is nearly ideal because the accuracy between training and testing differs by 1.5% and both accuracies are higher than 96%. This helps to reduce overfitting and minimize the misclassification among colorectal tissues. Hence, the effectiveness of the proposed technique is improved. The developed method attained Accr of 96.80%, Spec of 99.76%, Prec of 97.12%, Sens of 96.64%, F1 score of 0.9688, and AUC of 0.9820. It can be seen from Table 3 that the proposed network achieved more effectiveness in comparison to other existing techniques.

Table 3. Performance evaluation of proposed network and existing methods on the same dataset.

Authors	Method	Accr (%)	Prec (%)	Sens (%)	Spec (%)	F1 score	AUC
Kather et al. [26]	TL	94.30	94.33	92.33	99.44	—	**0.9950**
Liang et al. [6]	MFFCNN	96.00	97.42	94.50	98.90	0.9554	0.9600
Ghosh et al. [22]	EDNN	96.16	96.17	96.15	96.17	0.9610	0.9616
Kumar et al. [25]	CRCCN-Net	96.26	96.44	96.34	99.52	0.9638	0.9800
Proposed	**1D MHCNN**	**96.80**	**97.12**	**96.64**	**99.76**	**0.9688**	0.9820

5. Conclusion

Automated classification of colorectal tissue utilizing histopathological images may assist clinicians in making their decisions. This study classified colorectal tissue histological images into multiple classes. To do this, unique hand-crafted features were formulated utilizing the concatenation of image, SIFT, and 2D mel-cepstrum domain features. The resultant concatenated features consist of spatial and spectral information, which can extract more detailed information from unbalanced datasets of histopathological images. The concatenated features were then given as input to the proposed 1D MHCNN to classify colorectal tissue histopathological images. The experimental findings demonstrated that the proposed method has better Accr, Spec, Prec, Sens, and F1 score in comparison to other existing methods. The proposed method attained Accr of 96.80%, Spec of 99.76%, Prec of 97.12%, Sens of 96.64%, F1 score of 0.9688, and AUC of 0.9820.The performance of the proposed MHCNN can be extended using other optimization techniques. The proposed method may assist pathologists in improved clinical judgments and enable researchers to look into new possibilities for the study of colorectal cancer. Clinicians may set up the proposed MHCNN in hospitals to confirm diagnoses. In the future, the performance of the proposed methods will be validated for other challenging datasets related to colorectal cancer. The proposed technique will also be validated to diagnose various types of cancer such as skin, prostate, liver, breast, and lung among other health-related issues.

Conflict of interest

The authors confirm that they do not have any competing interests.

References

[1] Ferlay J, Colombet M, Soerjomataram I, Parkin DM, Piñeros M et al. Cancer statistics for the year 2020: an overview. International Journal of Cancer 2021; 149 (4): 778-789. https://doi.org/10.1002/ijc.33588

[2] Siegel RL, Miller KD, Wagle NS, Jemal A. Cancer statistics, 2023. CA: A Cancer Journal for Clinicians 2023; 73 (1): 17-48. https://doi.org/ 10.3322/caac.21763

[3] Gschwantler M, Kriwanek S, Langner E, Göritzer B, Schrutka-Kölbl et al. High-grade dysplasia and invasive carcinoma in colorectal adenomas: a multivariate analysis of the impact of adenoma and patient characteristics. European Journal of Gastroenterology & Hepatology 2002; 14 (2): 183-188. https://doi.org/10.1097/00042737-200202000-00013

[4] Jia X, Mai X, Cui Y, Yuan Y, Xing X et al. Automatic polyp recognition in colonoscopy images using deep learning and two-stage pyramidal feature prediction. IEEE Transactions on Automation Science and Engineering 2020; 17 (3): 1570-1584. https://doi.org/10.1109/TASE.2020.2964827

[5] Litjens G, Kooi T, Bejnordi BE, Setio AA, Ciompi F et al. A survey on deep learning in medical image analysis. Medical Image Analysis 2007; 42: 60-88. https://doi.org/10.1016/j.media.2017.07.005

[6] Liang M, Ren Z, Yang J, Feng W, Li B. Identification of colon cancer using multi-scale feature fusion convolutional neural network based on shearlet transform. IEEE Access 2020; 8: 208969-208977. https://doi.org/10.1109/ACCESS.2020.3038764

[7] Spanhol FA, Oliveira LS, Petitjean C, Heutte L. A dataset for breast cancer histopathological image classification. IEEE Transactions on Biomedical Engineering 2015; 63(7): 1455-1462. https://doi.org/10.1109/TBME.2015.2496264

[8] Gurcan MN, Boucheron LE, Can A, Madabhushi A, Rajpoot NM et al. Histopathological image analysis: a review. IEEE Reviews in Biomedical Engineering 2009; 2: 147-171. https://doi.org/10.1109/RBME.2009.2034865

[9] Takamatsu M, Yamamoto N, Kawachi H, Chino A, Saito S et al. Prediction of early colorectal cancer metastasis by machine learning using digital slide images. Computer Methods and Programs in Biomedicine 2019; 178: 155-161. https://doi.org/10.1016/j.cmpb.2019.06.022

[10] Weis CA, Kather JN, Melchers S, Al-Ahmdi H, Pollheimer MJ et al. Automatic evaluation of tumor budding in immunohistochemically stained colorectal carcinomas and correlation to clinical outcome. Diagnostic Pathology 2018; 13: 64. https://doi.org/10.1186/s13000-018-0739-3

[11] Alzubaidi L, Zhang J, Humaidi AJ, Al-Dujaili A, Duan Y et al. Review of deep learning: concepts, CNN architectures, challenges, applications, future directions. Journal of Big Data 2021; 8: 1-74. https://doi.org/10.1186/s40537-021-00444-8

[12] Shaban M, Awan R, Fraz MM, Azam A, Tsang YW et al. Context-aware convolutional neural network for grading of colorectal cancer histology images. IEEE Transactions on Medical Imaging 2020; 39 (7): 2395-2405. https://doi.org/10.1109/TMI.2020.2971006

[13] Kwak MS, Lee HH, Yang JM, Cha JM, Jeon JW et al. Deep convolutional neural network-based lymph node metastasis prediction for colon cancer using histopathological images. Frontiers in Oncology 2021; 10: 619803. https://doi.org/10.3389/fonc.2020.619803

[14] Altunbay D, Cigir C, Sokmensuer C, Gunduz-Demir C. Color graphs for automated cancer diagnosis and grading. IEEE Transactions on Biomedical Engineering 2009; 57 (3): 665-674. https://doi.org/10.1109/TBME.2009.2033804

[15] Olgun G, Sokmensuer C, Gunduz-Demir C. Local object patterns for the representation and classification of colon tissue images. IEEE Journal of Biomedical and Health Informatics 2013; 18 (4): 1390-1396. https://doi.org/10.1109/JBHI.2013.2281335

[16] Rathore S, Hussain M, Khan A. Automated colon cancer detection using hybrid of novel geometric features and some traditional features. Computers in Biology and Medicine 2015; 65: 279-296. https://doi.org/10.1016/j.compbiomed.2015.03.004

[17] Zhao D, Liu H, Zheng Y, He Y, Lu D et al. A reliable method for colorectal cancer prediction based on feature selection and support vector machine. Medical & Biological Engineering & Computing 2019; 57: 901-912. https://doi.org/10.1007/s11517-018-1930-0

[18] Masud M, Sikder N, Nahid AA, Bairagi AK, AlZain MA. A machine learning approach to diagnosing lung and colon cancer using a deep learning-based classification framework. Sensors 2021; 21 (3): 748. https://doi.org/10.3390/s21030748

[19] Sirinukunwattana K, Raza SE, Tsang YW, Snead DR, Cree IA et al. Locality sensitive deep learning for detection and classification of nuclei in routine colon cancer histology images. IEEE Transactions on Medical Imaging 2016; 35 (5): 1196-1206. https://doi.org/10.1109/TMI.2016.2525803

[20] Yazdi M, Erfankhah H. Multiclass histology image retrieval, classification using Riesz transform and local binary pattern features. Computer Methods in Biomechanics and Biomedical Engineering: Imaging & Visualization 2020; 8 (6): 595-607. https://doi.org/10.1080/21681163.2020.1761885

[21] Wang C, Shi J, Zhang Q, Ying S. Histopathological image classification with bilinear convolutional neural networks. In: 39th Annual International Conference of the IEEE Engineering in Medicine and Biology Society; Jeju Island, Korea; 2017. pp. 4050-4053. https://doi.org/10.1109/EMBC.2017.8037745

[22] Ghosh S, Bandyopadhyay A, Sahay S, Ghosh R, Kundu I et al. Colorectal histology tumor detection using ensemble deep neural network. Engineering Applications of Artificial Intelligence 2021; 100: 104202. https://doi.org/10.1016/j.engappai.2021.104202

[23] Hamida AB, Devanne M, Weber J, Truntzer C, Derangère V et al. Deep learning for colon cancer histopathological images analysis. Computers in Biology and Medicine 2021; 136: 104730. https://doi.org/10.1016/j.compbiomed.2021.104730

[24] Ohata EF, Chagas JV, Bezerra GM, Hassan MM, de Albuquerque VH et al. A novel transfer learning approach for the classification of histological images of colorectal cancer. Journal of Supercomputing 2021; 77: 9494-9519. https://doi.org/10.1007/s11227-020-03575-6

[25] Kumar A, Vishwakarma A, Bajaj V. Crccn-net: Automated framework for classification of colorectal tissue using histopathological images. Biomedical Signal Processing and Control 2023; 79: 104172. https://doi.org/10.1016/j.bspc.2022.104172

[26] Kather JN, Krisam J, Charoentong P, Luedde T, Herpel E et al. Predicting survival from colorectal cancer histology slides using deep learning: a retrospective multicenter study. PLoS Medicine 2019; 16 (1): e1002730. https://doi.org/10.1371/journal.pmed.1002730

[27] Kather JN, Halama N, Marx A. 100,000 histological images of human colorectal cancer and healthy tissue [dataset]. Zenodo 2018; 5281. https://doi.org/10.5281/zenodo.1214456

[28] Buades A, Coll B, Morel JM. A non-local algorithm for image denoising. In: 2005 IEEE Computer Society Conference on Computer Vision and Pattern Recognition; San Diego, CA, USA; 2005. pp. 60-65. https://doi.org/10.1109/CVPR.2005.38

[29] Liu H, Yang C, Pan N, Song E, Green R. Denoising 3D MR images by the enhanced non-local means filter for Rician noise. Magnetic Resonance Imaging 2010; 28 (10): 1485-1496. https://doi.org/10.1016/j.mri.2010.06.023

[30] Lowe DG. Distinctive image features from scale-invariant keypoints. International Journal of Computer Vision 2004; 60: 91-110.

[31] Oppenheim AV, Schafer RW. From frequency to quefrency: a history of the cepstrum. IEEE Signal Processing Magazine 2004; 21 (5): 95-106. https://doi.org/10.1109/MSP.2004.1328092

[32] Lee SK, Ho YS. Digital audio watermarking in the cepstrum domain. IEEE Transactions on Consumer Electronics 2000; 46 (3): 744-750. https://doi.org/10.1109/30.883441

[33] Kwon S. MLT-DNet: Speech emotion recognition using 1D dilated CNN based on multi-learning trick approach. Expert Systems with Applications 2021; 167: 114177. https://doi.org/10.1016/j.eswa.2020.114177

[34] Lella KK, Pja A. Automatic COVID-19 disease diagnosis using 1D convolutional neural network and augmentation with human respiratory sound based on parameters: cough, breath, and voice. AIMS Public Health 2021; 8 (2): 240. https://doi.org/10.3934/publichealth.2021019

[35] Kiranyaz S, Avci O, Abdeljaber O, Ince T, Gabbouj M et al. 1D convolutional neural networks and applications: a survey. Mechanical Systems and Signal Processing 2021; 151: 107398. https://doi.org/10.1016/j.ymssp.2020.107398

[36] Kumar A, Vishwakarma A, Bajaj V. An efficient convolutional neural network for classification of multi-class colorectal tissue using histopathological images. In: 2022 IEEE 6th Conference on Information and Communication Technology; Gwalior, India; 2022. pp. 1-5. IEEE. https://doi.org/10.1109/CICT56698.2022.9997889

[37] Kumar A, Vishwakarma A, Bajaj V, Sharma A, Thakur C. Colon cancer classification of histopathological images using data augmentation. In: 2021 International Conference on Control, Automation, Power and Signal Processing; Jabalpur, India; 2021. pp. 1-5. IEEE. https://doi.org/10.1109/CAPS52117.2021.9730704